Alternating current-to-direct current power conversion by single-wall carbon nanotube diodes

Govind Mallick,[1] Mark H. Griep,[1] Pulickel M. Ajayan,[2] and Shashi P. Karna[1,a)]
[1]*Department of the Army, U.S. Army Research Laboratory–Weapons and Materials Research Directorate, 4600 Deer Creek Loop, Aberdeen Proving Ground, Maryland 21005-5069, USA*
[2]*Department of Mechanical Engineering and Materials Science, Rice University, 6100 S. Main Street, Houston, Texas 77005, USA*

(Received 1 March 2010; accepted 16 April 2010; published online 9 June 2010)

We report the observation of alternating current-to-direct current half-wave conversion in the range of 1–1000 Hz by single-wall carbon nanotube diode rectifiers, which show a high degree of rectification ($\sim 10^5$). The nanoscale diode rectifier demonstrates a half-wave power conversion efficiency of 20%, which is comparable to that reported for larger metal oxide semiconductor field effect transistor diode designs. © *2010 American Institute of Physics*. [doi:10.1063/1.3429587]

Increasing demand for low power consumption and continued miniaturization of electronic device components in today's analog/digital circuits have reduced the supply voltage to sub-1 V levels.[1] The supply voltage to integrated circuit devices are provided by alternating current to direct current (ac-dc) converters, which convert high frequency ac voltage to a conditioned dc output voltage at a given power level. Low-voltage ac-dc converters generally consist of a diode rectifier, which is often composed of several diodes, an inductor and capacitor.[2–4] The critical feature of the ac-dc diode converter is its high rectification, which allows large current to flow only in one direction or for one phase of the ac input. Carbon nanotubes (CNT) have emerged as a viable material for ultralow power electronics, with possible applications ranging from simple interconnects to diodes and active field effect transistors.[5–14] In this letter, we demonstrate ac-dc power conversion by catalytically chemical vapor deposited (CCVD) single-wall carbon nanotubes (SWCNT) diodes in multiple arrays of switching devices fabricated over a 15×15 mm^2 Si/SiO_2 substrate with varying channel lengths. Utilizing the high forward/reverse current ratio, we observe efficient ac-dc power conversion based on these SWCNT devices.

SWCNTs, grown under CCVD conditions[15,16] on a 100 nm thick thermal oxide layer of a highly doped (n-type) Si substrate were used in this experiment. The SWCNT diodes, as shown in the scanning electron microscope (SEM) image in Fig. 1(a), were fabricated by photolithographically depositing 100 nm layer of Au on a 10 nm thick Ti to serve as electrodes with varying source (S) and drain (D) separation [Fig. 1(b)]. A single substrate (chip) with an approximate size of 15×15 mm^2 comfortably housed about 135 devices. These include four different channel lengths (gaps) between the electrodes (S and D) of 3 μm, 5 μm, 7 μm, and 10 μm, respectively, with the dimension of each electrode pad of 250×250 μm^2. Each device was uniquely labeled by its respective channel length, row, and column [Fig. 1(a)]. The sample was annealed at 200 °C for 30 min in constant

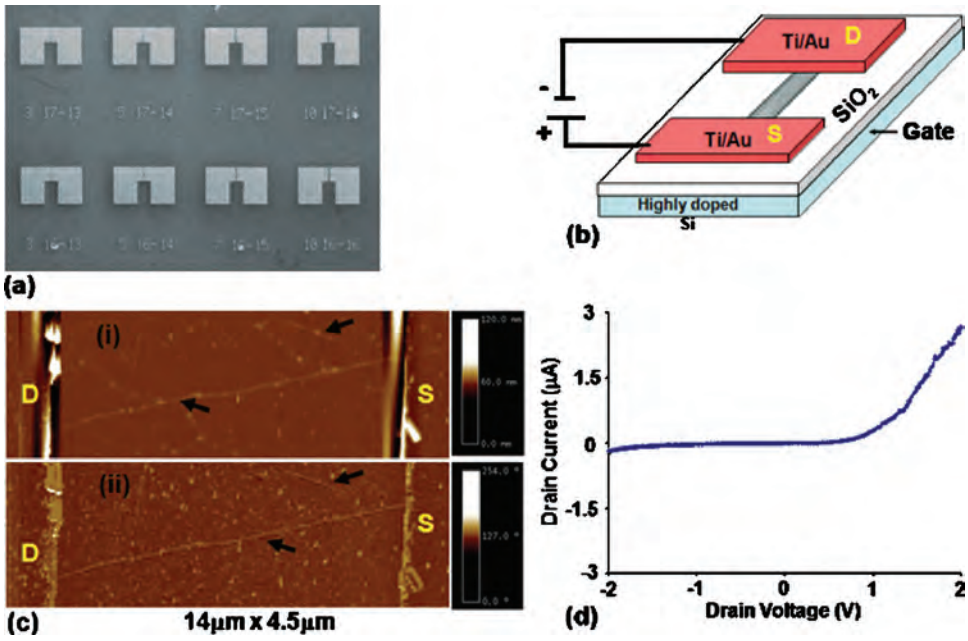

FIG. 1. (Color) (a) SEM image of 3, 5, 7, and 10 μm gap SWCNT-FET devices. The eight out of 135 devices on a 15×15 mm^2 substrate are distinctly marked and have the following coordinates. Rows: 16th and 17th; Column: 13th, 14th, 15th, and 16th, respectively. (b) Partial representation of the device assembly showing the schematic measurement of electrical properties. (c) Tapping mode AFM images showing SWCNTs connecting the electrodes [source (s) and drain (d)] of 10 μm gap device (i) height and (ii) phase. The CCVD grown SWCNTs are marked by arrows. (d) The drain current with respect to applied bias showing high I_{for}/I_{rev} ratio of the device.

a)Electronic mail: shashi.karna@us.army.mil.

Report Documentation Page

Form Approved
OMB No. 0704-0188

1. REPORT DATE	2. REPORT TYPE	3. DATES COVERED
APR 2010		**00-00-2010 to 00-00-2010**

4. TITLE AND SUBTITLE	5a. CONTRACT NUMBER
Alternating current-to-direct current power conversion by single-wall carbon nanotube diodes	5b. GRANT NUMBER
	5c. PROGRAM ELEMENT NUMBER
6. AUTHOR(S)	5d. PROJECT NUMBER
	5e. TASK NUMBER
	5f. WORK UNIT NUMBER
7. PERFORMING ORGANIZATION NAME(S) AND ADDRESS(ES) **U.S. Army Research Laboratory,Weapons and Materials Research Directorate,4600 Deer Creek Loop,Aberdeen Proving Ground,MD,21005-5069**	8. PERFORMING ORGANIZATION REPORT NUMBER
9. SPONSORING/MONITORING AGENCY NAME(S) AND ADDRESS(ES)	10. SPONSOR/MONITOR'S ACRONYM(S)
	11. SPONSOR/MONITOR'S REPORT NUMBER(S)

12. DISTRIBUTION/AVAILABILITY STATEMENT
Approved for public release; distribution unlimited

13. SUPPLEMENTARY NOTES

14. ABSTRACT

15. SUBJECT TERMS

16. SECURITY CLASSIFICATION OF:			17. LIMITATION OF ABSTRACT	18. NUMBER OF PAGES	19a. NAME OF RESPONSIBLE PERSON
a. REPORT **unclassified**	b. ABSTRACT **unclassified**	c. THIS PAGE **unclassified**	**Same as Report (SAR)**	**3**	

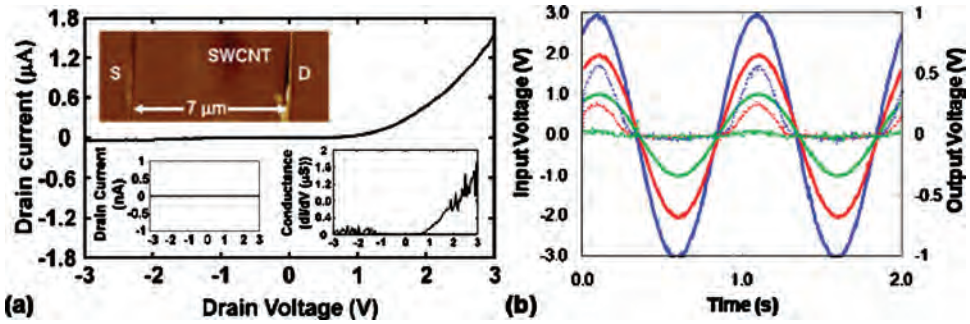

FIG. 2. (Color) (a) The *I-V* trace of a 7 μm gap device revealing the rectification behavior ($I_{for}/I_{rev} \sim 10^5$). The upper inset is the partial AFM image of the device showing SWCNT connecting the two electrodes. The lower right inset is the conductance (dI/dV) plot of the above *I-V* graph which shows significantly high conduction at the positive bias. The lower left inset is the *I-V* trace of a blank 7 μm gap device. (b) The corresponding experimental ac-to-dc half-wave conversion of 1 Hz ac inputs/dc output at 1 V (green solid/dashed), 2 V (red solid/dashed), and 3 V (blue solid/dashed), respectively.

flow of nitrogen to eliminate any surface oxygen defects. SEM, Hitachi S-4700 and atomic force microscope (AFM: Veeco CP-II) instruments were used to locate the bridging CNTs between the electrodes under ambient conditions and to measure the channel length (gap difference). Figure 1(c) shows the noncontact mode AFM (i) height and (ii) phase images of bundle of SWCNTs connecting a 10 μm gap device. The tubes, as indicated by the arrows in Fig. 1(c), are $\sim$2 nm in height and $\sim$50 nm in width,[17] suggesting bundles rather than isolated tubes consisting of multiple SWCNTs aligned parallel to each other. The electrical properties of the assembled devices were probed by a semiconductor (SC) analyzer (Keithley-4200) attached to a four-probe micromanipulated cryogenic system (Janis). Of the 135 fabricated devices, 103 were probed, of which 35% were found to be active. Out of the active devices 61% of 3 μm gap, 28% of 5 μm gap, 22% of 7 μm gap, and 26% of 10 μm gap devices were found active, i.e., they showed measurable electrical characteristics. Of the active devices, 72% showed asymmetric *I-V* curves and rest were either metallic or showed no observable electrical activity due to lack of connecting tubes. Out of the 72% asymmetric devices, the magnitude of forward/reverse current (I_{for}/I_{rev}) ratio ranged between 10^3 and 10^5. Figure 1(d) shows the measured *I-V* curve for the 10 μm gap device labeled "10 17–16," as shown in the SEM image of Fig. 1(a). A significantly high I_{for}/I_{rev} ratio ($\sim 10^5$) can be seen in the measured *I-V* curve.

The ac-to-dc power conversion by the SWCNT diodes was explored on the SC analyzer using the four-probe micromanipulator to make contact with the device source/drain pads. The source pad of the device was wired to a pulse generator (Agilent 81110) to provide an ac input signal of controlled frequency, amplitude, and waveform. For lower input frequencies, <1 Hz, the drain pad of the SWCNT device was connected to the SC analyzer for measurement of the output signal. The output measurements for higher input frequencies were performed on a high sampling rate oscilloscope (Agilent 54621A, 1 MΩ input resistance).

Figure 2 shows a typical *I-V* curve and corresponding ac-dc half-wave power conversion of 1–3 V at 1 Hz of a fabricated SWCNT device obtained from a two-probe measurement. The *I-V* curve shown is for a 7 μm channel length device (upper inset: tapping mode AFM image). The SWCNT diodes give high throughput of current in the forward bias [Fig. 2(a)]. The I_{for}/I_{rev} ratio at $+/-2$ V bias is on the order of $\sim 10^5$. The high I_{for}/I_{rev} ratio is also evident in the lower right inset of conductance (dI/dV) plot, which shows a significant increase in conduction with positive bias voltage.

The diodelike property of the as-grown SWCNT bundles most probably results from the structural defects on the SWCNT walls and presence of tubes with mixed chirality in the bundles.[17] The channel length or the number of nanotubes in any particular channel appears to have little or no effect on the rectification behavior. The lower left inset is the *I-V* curve on a 7 μm channel length control device with no SWCNT in the channel, showing no current. While most of the devices with different channel lengths showed rectification behavior, the dependence of rectification on the SC properties of the nanotube channel is not clear, and requires further investigation.

The half-wave power conversion of a 1, 2, and 3 V, and 1 Hz ac input is shown in Fig. 2(b). It can be seen that the negative voltage component of the input signal is nearly completely rectified and only the positive component passes through the SWCNT-device. With the 3 V ac input, for example, the device passes 20.1% of the positive ac-component and only 2.5% of the negative ac. Similar half-wave power conversion characteristics are seen over input frequencies ranging from 1 to 1000 Hz (Fig. 3). For practical applications, the efficiency of the device at a 60 Hz ac input signal is important. Half-wave power conversion of the SWCNT-FET rectifier device at 60 Hz, under multiple ac voltage loads, is shown in Fig. 4. As can be seen, similar to the 1 Hz ac input, the output voltage corresponding to the positive ac component is approximately 20% of the input voltage magnitude, compared to the $\sim$2% voltage conversion in the

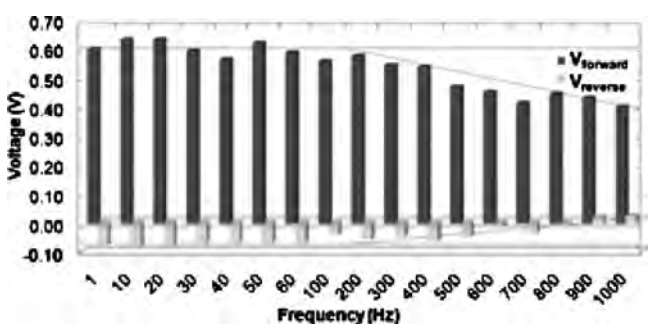

FIG. 3. ac-dc half-wave power conversion characteristics for input frequencies ranging from 1 to 1000 Hz. The reverse voltage is negligible compared to the forward voltage.

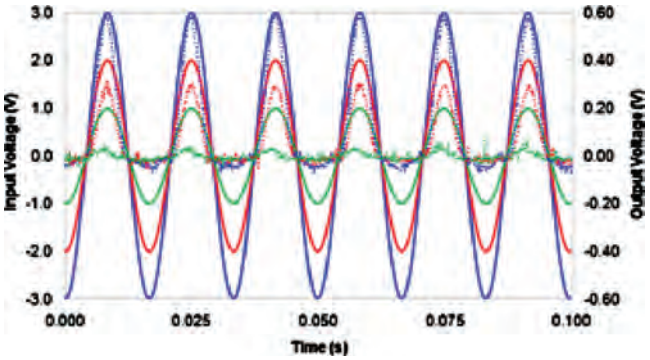

FIG. 4. (Color) ac-dc half-wave power conversion of the SWCNT-FET device at 60 Hz with ac inputs/dc output at 1 V (green solid/dashed), 2 V (red solid/dashed), and 3 V (blue solid/dashed), respectively.

negative component, which correlates to the rectification behavior of the SWCNT.

The ac-dc conversion characteristics of this device remain relatively unchanged over the tested range of 1–200 Hz (Fig. 3). However, in the ac-input frequency range of 200–1000 Hz, a distinct drop in the dc output voltage was seen. Since the input frequencies studied here were too low to contribute greatly to any capacitive or inductive effects, it is possible that the altered dc outputs are possibly the result of Joule heating at the SWCNT junction.[18,19] A higher frequency at 3 V ac input is expected to further elevate the Joule heating effect and decrease the heat dissipation period, resulting in an increased diode junction resistance and lowered current output, as observed.

In the 3 V input range, the half-wave power conversion efficiency (PCE) of the SWCNT diode is directly comparable to the 20%–25% PCE reported by complimentary metal oxide semiconductor (CMOS) and metal oxide semiconductor field effect transistor diodes.[20] To overcome this low efficiency, current CMOS designs employ complex integrated circuitry and active elements to minimize the cross-diode voltage drop, allow for full-wave conversion, and to reduce substrate leakage to realize efficiencies greater than 90%.[21,22] These same concepts are amenable to the smaller SWCNT diode and future designs can be engineered to maximize PCE with a reduced number of components and chip size.

In summary, ac-dc half-wave power conversion by SWCNT diodes with minimum components on the device is demonstrated. Advantage is taken of the nearly five orders of magnitude difference in the magnitude of the current of the diodes between the forward and backward biases. The minimum number of components in the demonstrated rectifier combined with a relatively easy device fabrication process makes it a highly attractive technology for engineering ac-dc power converters for low-power microelectronics and nanoelectronics devices.

All the authors listed have equally contributed to this research. This research was supported by the U.S. Army Research Laboratory, Director's Research Initiatives, Grant Nos. ARL-DRI-07-WMR-10 and ARL-DRI-08-WMR-20. P.M.A. acknowledges support from Rice faculty startup funding. We thank Sarah Lastella and Sangeeta Sahoo for help with the SWCNT growth and Gary Hirsch for SEM micrographs.

[1]W. Arden, P. Cogez, M. Graef, H. Ishiuchi, T. Osada, J. T. Moon, J. Roh, M. Liang, C. H. Diaz, P. Apte, B. Doering, and P. Gargini, The International Technology Roadmap for Semiconductors (ITRS) - 2008 update (overview), pp. 9–25 (http://www.itrs.net/Links/2008ITRS/Home2008.html).
[2]D. Rendusara, A. Jouanne, P. Enjeti, and D. A. Paice, IEEE Trans. Ind. Appl. **32**, 1293 (1996).
[3]D. Alexa, A. Sirbu, and A. Lazar, IEEE Trans. Ind. Electron. **53**, 1612 (2006).
[4]J. Chen, C. Kung, and Y. Hwang, IET Circuits Devices Syst **3**, 161 (2009).
[5]T. Ebbesen, H. Lezec, H. Hiuara, J. Bennett, H. Ghaemi, and T. Thio, Nature (London) **382**, 54 (1996).
[6]P. Collins, A. Zettl, H. Bando, A. Thess, and R. Smalley, Science **278**, 100 (1997).
[7]S. J. Tans, A. R. M. Verschueren, and C. Dekker, Nature (London) **393**, 49 (1998).
[8]R. Martel, T. Schmidt, H. Shea, T. Hertel, and P. Avouris, Appl. Phys. Lett. **73**, 2447 (1998).
[9]Z. Yao, C. Kane, and C. Dekker, Phys. Rev. Lett. **84**, 2941 (2000).
[10]T. Rueckes, K. Kim, E. Joselevich, G. Tseng, C. Cheung, and C. Lieber, Science **289**, 94 (2000).
[11]B. Satishkumar, P. John Thomas, A. Govindraj, and C. Rao, Appl. Phys. Lett. **77**, 2530 (2000).
[12]S. Heinze, J. Tersoff, R. Martel, V. Derycke, J. Appenzeller, and Ph. Avouris, Phys. Rev. Lett. **89**, 106801 (2002).
[13]Z. Zhong, D. Wang, Y. Cui, M. W. Bockrath, and C. M. Lieber, Science **302**, 1377 (2003).
[14]K. Jensen, J. Weldon, H. Garcia, and A. Zettl, Nano Lett. **7**, 3508 (2007).
[15]S. Lastella, G. Mallick, R. Woo, D. Rider, I. Manners, Y. Jung, C. Ryu, P. Ajayan, and S. P. Karna, J. Appl. Phys. **99**, 024302 (2006).
[16]S. Lastella, Y. Joon Jung, H. Yang, R. Vajtai, P. Ajayan, C. Ryu, D. Rider, and I. Manners, J. Mater. Chem. **14**, 1791 (2004).
[17]G. Mallick, M. Griep, S. Lastella, S. Sahoo, S. Hirsch, P. Ajayan, and S. Karna, J. Nanosci. Nanotechnol. **10**, 1 (2010).
[18]P. Vincent, S. Purcell, C. Journet, and V. Binh, Phys. Rev. B **66**, 075406 (2002).
[19]J. Kong, C. Zhou, A. Morpurgo, H. Soh, C. Qhate, C. Marcus, and H. Dai, Appl. Phys. A: Mater. Sci. Process. **69**, 305 (1999).
[20]C. Peters, O. Kessling, F. Henrici, M. Ortmanns, and Y. Manoli, Proceedings of the IEEE International Symposium on Circuits and Systems (ISCAS), 2007 (unpublished), pp. 2415–2418.
[21]C. Peters, D. Spreemann, M. Ortmanns, and Y. Manoli, J. Micromech. Microeng. **18**, 104005 (2008).
[22]G. Bawa and M. Ghovanloo, Analog. Integr. Circ. Sig. Process **60**, 71 (2009).